

Supplementary Materials

1. Detector Filter and Acquisition Rates

It has been previously shown that at high flow rates, the settings on the detector and signal filter can modify the observed peak shape [1]. To that end, we determined the appropriate experimental filter rate on the Stanford Research Systems SR750 current amplifier (Section 3.2) by varying some of the possible settings (the data acquisition rate was kept constant at 80 Hz to ensure sufficiency sampling of the measured peak). In Figure S1, it is clear that a 30 Hz filter rate reduces additional broadening due to detection (especially at high flow rates and fast runs used for peak profile observations discussed in Section 4.4). Because of this, all experimental data was collected at this filter rate so that broadening due to detector settings was negligible.

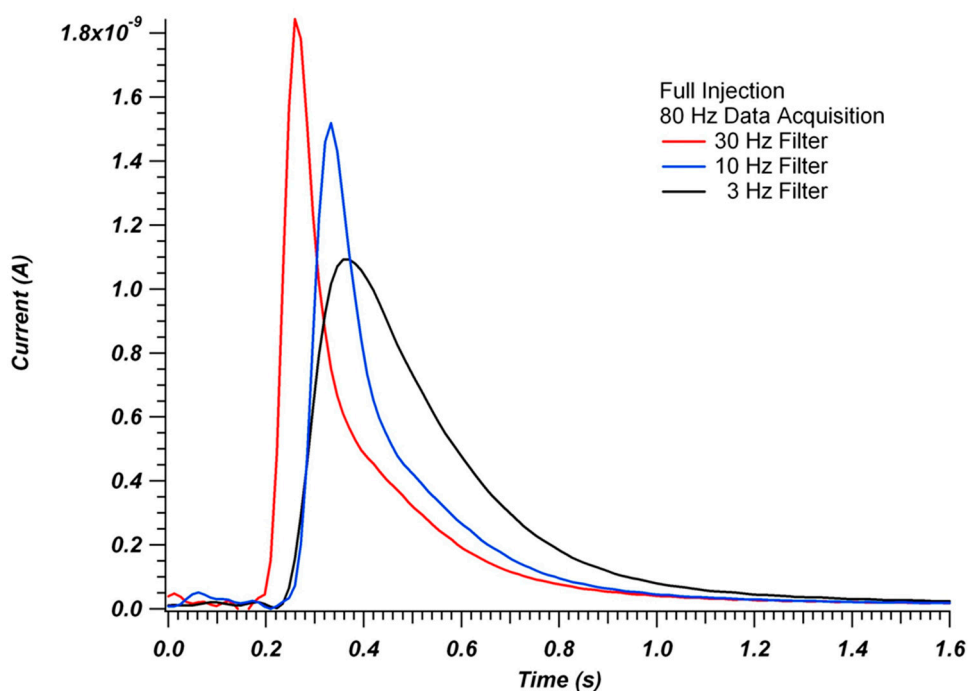


Figure S1. Measurement of 4-methyl catechol through a 6 cm, 13 μm i.d. capillary using a carbon fiber electrode detector with a full loop injection. Data acquisition rate was set at 80 Hz and preamplifier filter rates were set to 3, 10, and 30 Hz.

2. Characterization of Peaks for Variance Calculations

To effectively use the Foley-Dorsey EMG peak fitting model [2–4] to characterize peak variance (and separate sigma-type and tau-type broadening contributions), the peak fits must match relatively well with the measured peak at the end of the injector-tube system. The raw data, fits generated by the EMG function in Igor Pro 6.2, and residuals between the two are overlaid in Figure S2. In all cases, there are some residuals near the peak maximum. Additionally, there are higher residuals in the peak tail when tau is greater than sigma (Figure S2A) than when sigma is greater than tau (Figure S2B). However, in all cases the fit is relatively close to the raw data (maximum residuals are less than 5% of the peak height) and can be used to make a reasonable estimation of both sigma and tau (which is not accessible when using the ISM method).

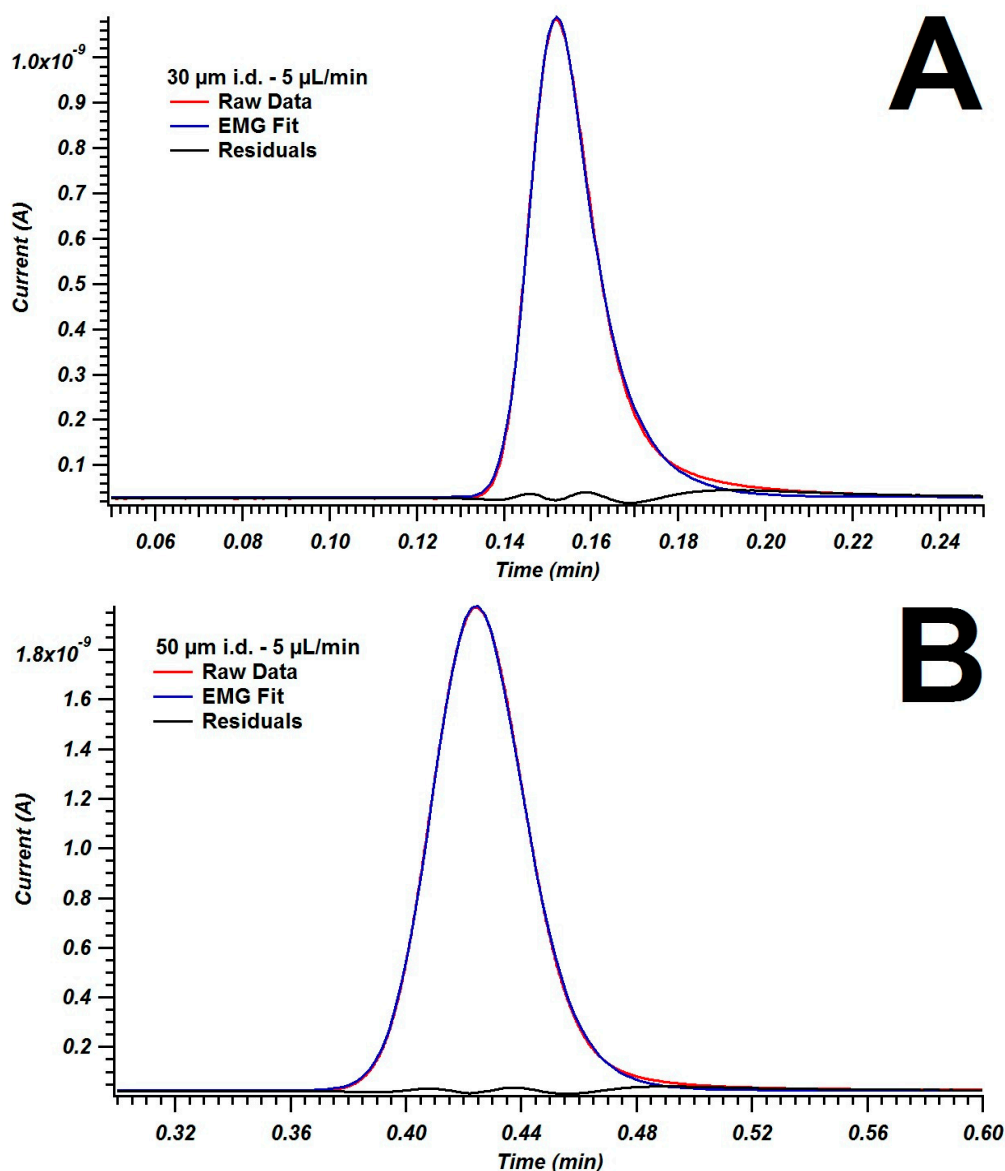


Figure S2. Measured peaks (red) and EMG fits to the experimental data (blue) and the residuals between the two (black) for a case where tau is greater than sigma (A, 30 μm i.d., 5 $\mu\text{L}/\text{min}$) and sigma is greater than tau (B, 50 μm i.d. 5 $\mu\text{L}/\text{min}$).

When trying to characterize peak variance, the most accurate method is traditionally the use of the second central moment [5–11]. In this experiment, we use an EMG function because it allows for the separation of sigma-type and tau-type broadening. To compare the two methods (variance in EMG is calculated as $\sigma^2 + \tau^2$ while the second central moment was calculated using the ISM method [12] with -3σ and $+5\sigma$ selected as initial integration boundaries to ensure the tail was fully encompassed), variance values for both are shown in Figure S3. They were compared with 20 μm i.d. data with a timed pinch injection (selected because they were the narrowest peaks for the entire data set and thus the most difficult to calculate for both ISM and EMG methods) and demonstrate the largest relative difference between the curves for different data sets. Since the focus of this report is on general trends that are found across flow rates and tubing diameters, the advantages of the EMG function for our purposes and the fact that the general curve shape is similar outweigh the difference in calculated variance (previous

studies of peak characterization in capillaries have also found good agreement between measured variance between the EMG and moments methods [13]).

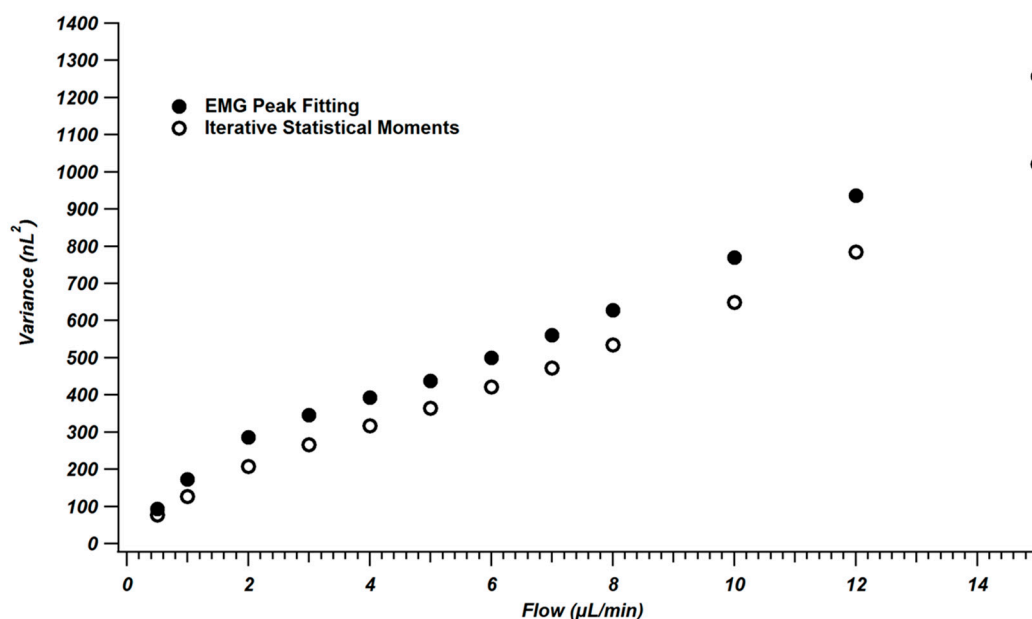


Figure S3. Variance values calculated using an EMG peak fit and an ISM algorithm (interval of -3σ , $+5\sigma$) for a 1 m, 20 μm i.d. capillary with a timed pinch injection.

3. Peak Signal with Pinched Injection Mode

In the pinched injection mode, the injection valve switches the internal loop into the flow path for 100 ms. While the full internal loop in the valve used in these experiments only holds 20 nL, at slower flow rates the entire loop may not be eluted during this short time switch. The theoretical volume that should be injected can be calculated by multiplying the flow rate by the valve switch time. These theoretical volumes are compared to estimated volumes that were observed experimentally in Figure S4. The experimental values were estimated by comparing the average peak area of injected peaks at a given flow rate using the pinch mode to the average peak area of peaks using the full injection at the same condition. These values were then compared and the full injection peak area was assumed to represent 20 nL. From these results, it was shown that at low flow rates (up to 8 $\mu\text{L}/\text{min}$) that the volume injected was greater than would be expected by 2–3 nL. At flow rates above 8 $\mu\text{L}/\text{min}$, the injected volume reaches a plateau at 17 nL. This data suggests that at the beginning of the valve pulse that more of the loop is injected and that after the switch, at least ~ 3 nL remains (even at the highest flow rates where this volume should be eluted from the loop). This is a key reason that the peak shapes improve when using this mode as this remaining volume is a key contributor to the tail end of the eluted band.

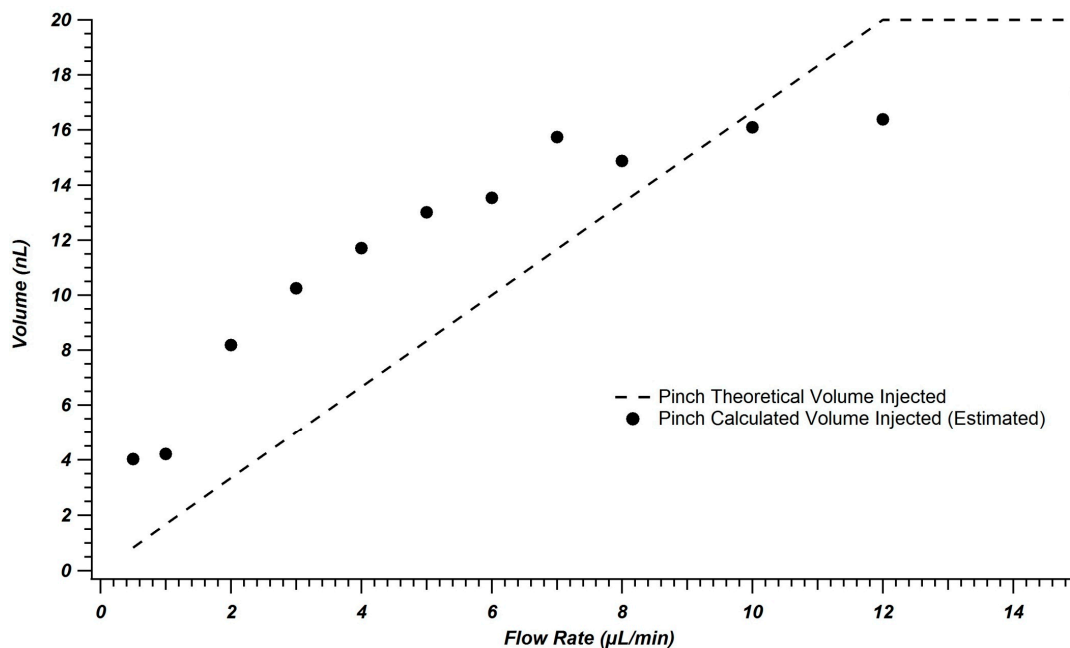


Figure S4. Comparison of the theoretical injected volume (based on flow rate, internal loop volume, and valve switch time) compared to the calculated injected volume (based on a peak area comparison between full and pinch injection modes) for the timed pinch injection mode.

References

1. Fountain, K.J.; Neue, U.D.; Grumbach, E.S.; Diehl, D.M. Effects of extra-column band spreading, liquid chromatography system operating pressure, and column temperature on the performance of sub-2-microm porous particles. *J. Chromatogr. A* **2009**, *1216*, 5979–5988.
2. Foley, J.P.; Dorsey, J.G. Equations for calculation of chromatographic figures of merit for ideal and skewed peaks. *Anal. Chem.* **1983**, *55*, 730–737.
3. Foley, J.P.; Dorsey, J.G. A Review of the Exponentially Modified Gaussian (EMG) Function: Evaluation and Subsequent Calculation of Universal Data. *J. Chromatogr. Sci.* **1984**, *22*, 40–46.
4. Jeansonne, M.S.; Foley, J.P. Review of the Exponentially Modified Gaussian (EMG) Function Since 1983. *J. Chromatogr. Sci.* **1991**, *29*, 258–266.
5. Sternberg, J.C. Extracolumn Contributions to Chromatographic Band Broadening. In *Advances in Chromatography*; Giddings, J., Keller, R.A., Eds.; Marcel Dekker: New York, NY, USA, 1966; Volume 2, pp. 205–270.
6. Grushka, E.; Myers, M.N.; Schettler, P.D.; Giddings, J.C. Computer characterization of chromatographic peaks by plate height and higher central moments. *Anal. Chem.* **1969**, *41*, 889–892.
7. Gritti, F.; Felinger, A.; Guiochon, G. Influence of the errors made in the measurement of the extra-column volume on the accuracies of estimates of the column efficiency and the mass transfer kinetics parameters. *J. Chromatogr. A* **2006**, *1136*, 57–72.
8. Gritti, F.; Guiochon, G. Accurate measurements of peak variances: Importance of this accuracy in the determination of the true corrected plate heights of chromatographic columns. *J. Chromatogr. A* **2011**, *1218*, 4452–4461.

9. Verstraeten, M.; Liekens, A.; Desmet, G. Accurate determination of extra-column band broadening using peak summation. *J. Sep. Sci.* **2012**, *35*, 519–529.
10. Stevenson, P.G.; Gao, H.; Gritti, F.; Guiochon, G. Removing the ambiguity of data processing methods: optimizing the location of peak boundaries for accurate moment calculations. *J. Sep. Sci.* **2013**, *36*, 279–287.
11. Stevenson, P.G.; Gritti, F.; Guiochon, G. Automated methods for the location of the boundaries of chromatographic peaks. *J. Chromatogr. A* **2011**, *1218*, 8255–8263.
12. Hsieh, S.; Jorgenson, J.W. Preparation and Evaluation of Slurry-Packed Liquid Chromatography Microcolumns with Inner Diameters from 12 to 33 μm . *Anal. Chem.* **1996**, *68*, 1212–1217.
13. Niessen, W.M.A.; van Vliet, H.P.M.; Poppe, H. Studies on external peak broadening in open-tubular liquid chromatography systems using the exponentially modified Gaussian model. *Chromatographia* **1985**, *20*, 357–363.